Neuron, Vol. 39, 701–711, August 14, 2003, Copyright ©2003 by Cell Press

Dissociation of Neural Representation of Intensity and Affective Valuation in Human Gustation

Dana M. Small,[1,2,3,4,6,*] Michael D. Gregory,[1,2] Y. Erica Mak,[1,2] Darren Gitelman,[1,2,3,5,6] M. Marsel Mesulam,[1,2,3] and Todd Parrish[1,2,3,5]
[1]Cognitive Neurology and Alzheimer's Disease Center
[2]Cognitive Brain Mapping Group
[3]Department of Neurology
[4]Department of Psychology
[5]Department of Radiology
[6]Northwestern University Institute for Neurosciences
Northwestern University Feinberg Medical School
320 East Superior Street
Chicago, Illinois 60611

Summary

We used a 2 × 2 factorial design to dissociate regions responding to taste intensity and taste affective valence. Two intensities each of a pleasant and unpleasant taste were presented to subjects during event-related fMRI scanning. The cerebellum, pons, middle insula, and amygdala responded to intensity irrespective of valence. In contrast, valence-specific responses were observed in anterior insula/operculum extending into the orbitofrontal cortex (OFC). The right caudolateral OFC responded preferentially to pleasant compared to unpleasant taste, irrespective of intensity, and the left dorsal anterior insula/operculuar region responded preferentially to unpleasant compared to pleasant tastes equated for intensity. Responses best characterized as an interaction between intensity and pleasantness were also observed in several limbic regions. These findings demonstrate a functional segregation within the human gustatory system. They also show that amygdala activity may be driven by stimulus intensity irrespective of valence, casting doubt upon the notion that the amygdala responds preferentially to negative stimuli.

Introduction

Sensory systems must code for a variety of perceptual characteristics of sensory stimuli. In the gustatory system, the primary dimensions are quality (sweet, sour, salty, bitter, or savory), intensity, and affect (pleasant/unpleasant). These dimensions tend not to be orthogonal but interact so that subjects have considerable difficulty providing perceptual ratings of intensity independently from affective valence (Pfaffmann, 1980). For example, very weak concentrations of bitter-tasting solutions (negative valence) tend to be rated as quite intense, while strong concentrations of sweet-tasting solutions (positive valence) are rated as quite weak. However, if subjects are trained to rate stimulus concentration irrespective of valence (e.g., focus upon how bitter the solution is compared to other bitter solutions), many subjects are quite successful at using intensity to reflect stimulus concentration (Small et al., 2001b).

Although this "negative bias" for intensity (Carretie et al., 2001) appears to be common to all sensory modalities, Anderson and colleagues have argued that it is easier to achieve a dissociation between affect and intensity in the olfactory modality because stimuli are simple and relatively free from confounding semantic manipulations, which characterize many visual stimuli (e.g., pleasant and unpleasant visual scenes) (Anderson et al., 2003). Thus, they were able to successfully dissociate the perception of odor intensity from affective valence and found that activation in the amygdala was associated with intensity regardless of valence, whereas activity in the orbitofrontal cortex reflected valence irrespective of intensity. Although the orbitofrontal cortex is consistently implicated in affective processing of visual (LaBar et al., 2001; Morris et al., 1997; Stoleru et al., 1999), somatosensory (Apkarian et al., 1999, 2000, 2001; Francis et al., 1999), auditory (Blood and Zatorre, 2001; Blood et al., 1999), olfactory (O'Doherty et al., 2000; Royet et al., 2000; Zald and Pardo, 1997), gustatory (O'Doherty et al., 2001b, 2002; Zald et al., 1998, 2002), food (Berns et al., 2001; Small et al., 2001a), and abstractly rewarding stimuli (O'Doherty et al., 2001a; Thut et al., 1997), the notion that the amygdala codes for intensity rather than affective valence contrasts with a multitude of earlier reports of amygdala response to affectively laden stimuli (Baxter and Murray, 2002; Lane et al., 1997; Morris et al., 1997; O'Doherty et al., 2001a, 2001b, 2002; Royet et al., 2000; Small et al., 1997; Zald, 2003a; Zald et al., 1998, 2002; Zald and Pardo, 1997). However, the Anderson study differs from the vast majority of earlier studies in that intensity was independently manipulated and matched across affective valences.

In the current study, we sought to extend the findings of Anderson and colleagues to the gustatory modality and to include whole-brain coverage. To ensure that our stimuli were carefully equated for affect and intensity, subjects were brought into the chemosensory lab prior to scanning and asked to rate the intensity and pleasantness of several concentrations of sweet (pleasant) and bitter (unpleasant) solutions. Stimulus concentration was yoked independently for each subject so that ratings would fall within the targeted range (Figure 1). The results of ratings taken during scanning are illustrated in Figure 1 and show that the dissociation was maintained throughout the experiment with no habituation. In the scanner, intense pleasant (IP), intense unpleasant (IUP), weak pleasant (WP), weak unpleasant (WUP), and tasteless (O'Doherty et al., 2001b) solutions were delivered as 0.5 cc over a 5 s period with a cue to swallow occurring 15 s after stimulus onset (Figure 2). In accordance with Anderson and colleagues, we found that the amygdala was responsive to intensity irrespective of valence, whereas the orbitofrontal cortex was responsive to affective valence and not intensity. In addition,

*Correspondence: d-small@northwestern.edu

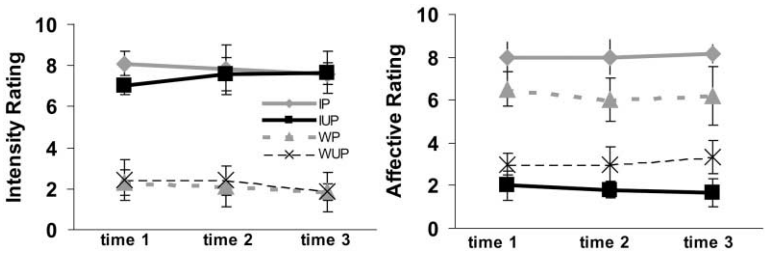

Figure 1. Mean Intensity and Affective Ratings over Time

Mean intensity (left) and affective (right) ratings across three time points (time 1, prior to first scan; time 2, following fourth scan [midexperiment]; time 3, after final scan). IP, intense pleasant; IUP, intense unpleasant; WP, weak pleasant; and WUP, weak unpleasant. Ratings were made on 11 point scales (Intensity: 0, no intensity; 3, weak; 7, strong; and 10, extremely intense. Pleasantness: 0, extremely unpleasant; 3, unpleasant; 5, neutral; 7, pleasant; and 10, extremely pleasant). Only subjects whose ratings fell within the targeted range in the screening session were asked to participate in the fMRI session (15/19). The targeted range was defined as intensity ratings of 8 ± 1 (intense) and 2 ± 1 (weak) for both solutions and a pleasantness rating of 8 ± 1 for the sweet solution and unpleasantness rating of 2 ± 1 for the bitter. Repeated measures analyses of variance indicated that ratings did not change over the duration of the fMRI experiment [$F(1,8)$ 0.8; $p = 0.39$] and that the affective ratings of the pleasant and unpleasant stimuli were significantly different [$F(1,8)$ 140; $p < 0.001$] as were the intense intensity ratings between the weak and the strong stimuli [$F(1,8)$ 795; $p < 0.001$]. In addition, the unpleasant stimuli were rated as equally intense across time ($p = 0.21$, 0.67, and 0.59, respectively) as were the weak stimuli ($p = 0.37$, 0.4, and 0.6). However, IP was rated as more pleasant than the WP at all times ($p = 0.001$, 0.003, 0.001) and IUP as more unpleasant than WUP ($p = 0.002$, 0.001, 0.003). Fortunately, the difference between the IP − WP and IUP − WUP did not differ [$F(1,8)$ 0.22; $p = 0.75$].

we describe a functional segregation within the human gustatory system with the cerebellum, brainstem, amygdala, and middle insula coding for intensity and the anteroventral insula, oribtofrontal cortex, and anterior cingulate cortex coding for affective valence.

Results

Data were analyzed with SPM99 (Wellcome Department of Neurology, London) using group random effects analyses and conjunction analyses within a fixed-effects model. Several different analyses were performed to address coding of each of the three main perceptual dimensions: intensity, pleasantness, and unpleasantness. We applied Gaussian random field theory as implemented in SPM99 (Friston et al., 1994; Worsley and Friston, 1995). This required using an initial t map threshold of $p = 0.001$ uncorrected. Areas were then considered significant if their associated clusterwise p value was $p < 0.05$ corrected across the entire brain volume for unpredicted peaks. For predicted peaks, a priori regions of interest were specified using the small volume correction (SVC) function (to the nearest cluster) in SPM99 (Worsley et al., 1996) and were considered significant if the corresponding voxelwise p value was less than 0.005 corrected for multiple comparisons.

Intensity Coding

To determine brain regions responding to taste intensity irrespective of affective valence, we first assessed the main effect of intensity [(IP + IUP) − (WUP + WP)], which produced activation bilaterally in the middle insula, pons and cerebellum, left substantia nigra, and right amygdala (Table 1, Figures 3, 4, and 5—green peaks). A conjunction analysis (based upon a fixed-effects model) was also performed to isolate responses that were greater in intense pleasant (IP) compared to weak pleasant (WP) and also greater in intense unpleasant (IUP) compared to weak unpleasant (WUP) [(IP − WP) and (IUP − WUP)]. This resulted in a very similar activation pattern as did the random effects analysis. In both intensity analyses, insular activations correspond well to the region identified as the putative primary gustatory area in humans (Figure 4) (Petrides and Pandya, 1994; Small et al., 1999). The amygdala activation was in a posterior region of the amygdala almost at the junction with the hippocampus (Figure 3). This is the same region that Anderson and colleagues reported correlated with ratings of odor intensity irrespective of valence (Anderson et al., 2003). Figure 3 shows the amygdala activations from the random effect analysis and from two representative subjects. The graphs of this figure clearly show that intensity rather than valence is driving the response in the amygdala. Notably, the weak unpleasant solution tended to be associated with a decrease in activation. Amygdala activation was also seen in IP − WUP (12, −12, 18; $z = 4.0$; $p = 0.0004$ SVC) and IUP − WP, following a region of interest analysis using a 5 mm sphere around the peak isolated in IUP − WUP ($p = 0.002$). Inspection of the results from the contrast of intense pleasant minus

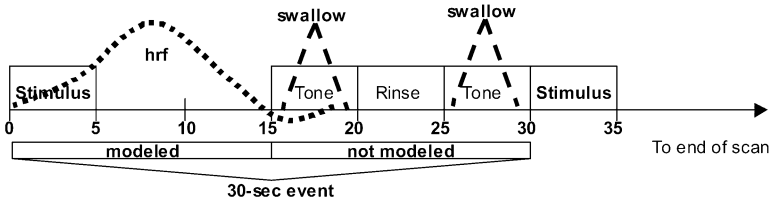

Figure 2. Graphic Depiction of Long Event-Related Design

A long-event related design was used to enable dissociation of the event of interest (tasting) from movement related to swallowing. Four different taste stimuli (IP, WP, IUP, WUP) and one tasteless stimulus (with similar ionic components to saliva; O'Doherty et al., 2001b) were delivered during the stimulus block. Events began with delivery of 0.5 cc solution over a 5 s period (stimulus). The liquid was held in the mouth until a 400 Hz tone played for 5 s signaling the window of time during which subjects were allowed to swallow. The tone was followed by a 5 s rinse, which was in turn followed by a second tone signaling that the subject should swallow again. The dotted line indicates the predicted hemodynamic response function (hrf). By signaling the subject to swallow 15 s after taste delivery, the peak of the hrf should be free from contamination by movement related to swallow. Only this hrf segment of the data is analyzed. Each stimulus was presented twice per run, and a total of eight runs were performed. Runs lasted for 5 min and 13 s (12.6 s to equilibrate).

Table 1. Results from Intensity Analyses

Brain Region	x	y	z	z Statistic	p Value (SVC)
(IP + IUP) − (WP + WUP)					
Cerebellum	−30	−48	−30	4.0	0.0002
	3	−45	−21	3.9	0.001
	−18	−57	−21	3.7	0.001
Pons	−12	−27	−36	5.2	0.00001
	−9	−39	−27	4.3	0.0001
	9	*−39*	−36	*4.1*	*0.0003*
	9	*−48*	*−30*	*4.1*	*0.0001*
	9	*−18*	*−21*	*3.7*	*0.001*
	6	−27	*−39*	3.5	0.002
Amygdala	15	−10	−15	3.6	0.001
Substantia nigra	−12	−12	−12	4.3	0.0001
Putamen	24	9	−12	3.9	0.0003
Insula/operculum	39	6	−6	3.9	0.008**
	42	*12*	*0*	*3.8*	*0.001*
	51	*6*	*−3*	*3.7*	*0.001*
	−45	0	0	3.8	0.001
	−33	3	12	3.7	0.001
Anterior cingulate	−9	0	51	3.6	0.001
IP − WP					
Cerebellum	3	−54	−18	3.7	0.001
Pons	6	−27	−39	4.1	0.0002
	−12	−27	−33	3.7	0.001
Amygdala	−24	−6	−21	2.9	0.007
	−12	−12	−21	2.8	0.008
Thalamus	21	−15	18	3.7	0.002
Insula/operculum	−45	9	6	3.8	0.001
Insula	36	9	−3	3.9	0.001
Posterior insula	−39	−30	24	3.4	0.004
Anterior cingulate cortex	3	−12	45	4.7	0.05**
	15	15	33	4.1	0.02**
	−6	−3	39	4.1	0.0002
	−15	24	30	3.7	0.0004
Temporal pole	−51	15	−21	3.5	0.001
IUP − WUP					
Cerebellum	−21	−57	−21	4.6	0.0001
	−21	*−66*	*−18*	*3.8*	*0.003*
	−33	−54	−30	4.1	0.0001
	3	−48	−12	3.6	0.001
	27	−45	−27	3.5	0.003
	18	*−42*	*−30*	*3.5*	*0.004*
	24	*−51*	*−33*	*3.3*	*0.004*
Pons	3	−36	−36	3.9	0.0003
	−9	−24	−36	3.4	0.001
Amygdala	27	−9	−12	4.0	0.001
Substantia nigra	−12	−12	−12	4.3	0.0003
Putamen	−21	0	6	3.7	0.001
	−30	0	−6	3.6	0.001
	−21	12	0	3.4	0.001
Insula/operculum	−42	27	0	3.7	0.001
	48	27	−12	3.6	0.001

SVC, small volume correction; **cluster p value corrected for entire brain. Italics indicate that a peak falls under the same cluster as the preceding peak.

weak pleasant (IP − WP) and intense unpleasant minus weak unpleasant (IUP − WUP) also isolated activation within the cerebellum, pons, amygdala, and middle insula (Table 1).

Pleasantness Coding

To ascertain regions of the brain responding preferentially to both intensities of the pleasant taste, we compared the mean activation of the weak and intense pleasant solutions (IP + WP) to the activation resulting from the tasteless condition [(IP + WP) − tasteless]. Activation was observed bilaterally in the caudolateral orbitofrontal cortex, as well as in the right thalamus, anterior ventral insula/caudal OFC, and ventral striatum (Table 2 and Figure 5—magenta peaks). Midline activations were observed in the hypothalamus and anterior and subcallosal cingulate cortex. Activation isolated in this analysis must be present to some extent in both intense pleasant (IP) and weak pleasant (WP). Analysis of the main effects of each of these conditions showed that this was indeed the case for the anteroventral insula (IP = 36, 12, −3; z = 3.4; p = 0.002 SVC; WP = −27, 12, −15; z = 3.3; p = 0.003 SVC), anterior cingulate (IP = 0, 39, 9; z = 4.5; p = 0.00003 SVC; WP = 0, 36, −3;

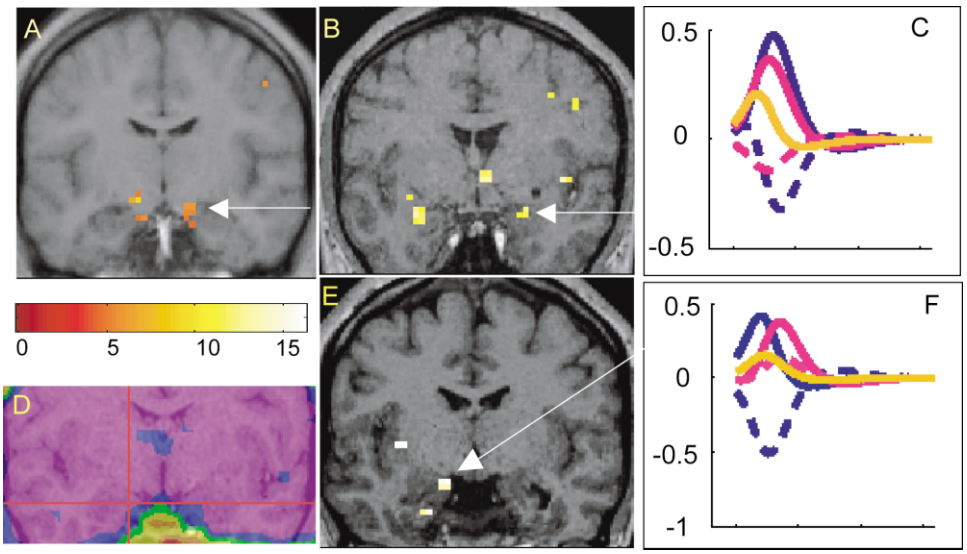

Figure 3. Amygdala Activations

Amygdala activation associated with intensity irrespective of affective valence in the analysis of (IP + IUP) − (WP + WUP) for the group random effects analysis, plotted onto the mean MRI image (A), and for two representative subjects, (B) and (E), plotted on their respective anatomical scans. In subject (B), activations occurred at −21, −12, −18 (z = 3.3; p = 0.003 after SVC) and 20, −10, −18 (z = 3.6; p = 0.001 after SVC) and in (E) at −9, −6, −12 (3.9; 0.0001 after SVC). The BOLD sensitivity map (D) (Parrish et al., 2000) from the subject shown in (E) is presented with the crosshair centered over the area of the amygdala where activation occurred (E). The BOLD detectability map shows our ability to detect 0.5% signal change within most of the amygdala. Purple indicates ability to detect a 0.5% signal change; blue, 1%; green, 2%; and yellow, 4%. Graphs on the right (C and F) show fitted hemodynamic response function extracted from peak activations indicated by the white arrow in each of the two representative subjects (*y* axis, response; *x* axis, peristimulus time with each line indicating a 5 s interval) to each of the five trial types (blue solid, IUP; blue dotted, WUP; magenta solid, IP; magenta dotted, WP; yellow solid, tasteless.)

z = 4.2; p = 0.00002; −9, 39, 0; z = 3.8; p = 0.002 SVC; 12, 42, 30; z = 4.0; p = 0.0004 SVC; 6, 57, 12; z = 3.4; p = 0.002 SVC), caudolateral orbitofrontal cortex (IP = −33, 18, −21; z = 3.5; p = 0.002 SVC; −33, 33, −21; z = 4.2; p = 0.0001 SVC; WP = 33, 33, −18; z = 4.6; p = 0.00009 SVC; −33, 24, −21; z = 3.8; p = 0.001 SVC), and ventral striatum (IP = −27, 9, −9; z = 4.0; p = 0.001 SVC; WP = −21, 3, 6; z = 3.4; p = 0.001 SVC; 30, 9, 3; z = 3.2; p = 0.002 SVC). Intense pleasant compared to intense unpleasant (IP − IUP) showed that the anterior cingulate cortex (−15, 33, 33; z = 4.2; p = 0.00008 SVC) and right caudolateral orbitofrontal cortex (39, 33, −15; z = 3.2; p = 0.007 SVC) responded preferentially to pleasant compared to unpleasant intense taste. The right caudolateral orbitofrontal cortex was also activated in the comparison of intense pleasant to weak unpleasant (IP − WUP = 39, 33, −9; z = 3.7; p = 0.002 SVC), weak pleasant to weak unpleasant (WP − WUP = 39, 31, −15; z = 3.5; p = 0.001 SVC), and in a region of interest analysis (using a 5 mm sphere from the peak from IP − IUP) collapsing across intensity [(IP + WP) − (IUP + WUP)] (p = 0.001), strongly suggesting that it is activated preferentially by pleasant compared to unpleasant taste, irrespective of intensity. The anterior cingulate cortex was also preferentially activated in a region of interest analysis using a 5 mm sphere from the peak identified in [(IP + WP) − tasteless] (0, 39,6) in the comparison [(IP + WP) − (IUP + WUP)] (p = 0.0004).

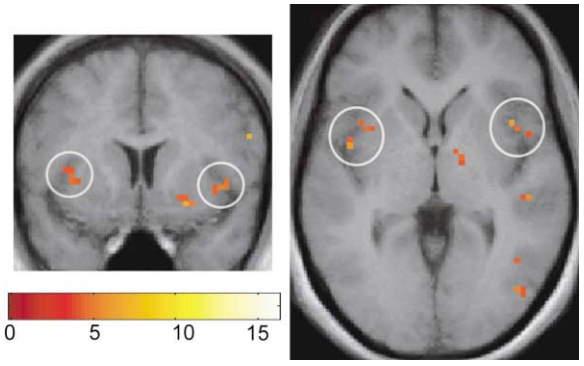

Figure 4. Regions of the Insular Responding to Intensity

Bilateral activation in the insula as a main effect of intensity [(IP + IUP) − (WP + WUP)] (peaks circled are reported in Table 1 under insula).

Unpleasantness Coding

To uncover regions of the brain responding preferentially to both concentrations of unpleasant taste, we compared the mean activation of the weak and intense unpleasant solutions (IUP + WUP) to the activation resulting from the tasteless condition [(IP + WP) − tasteless]. This produced activation in the midbrain, putamen, hypothalamus, claustrum, anterior insula/operculum, orbitofrontal cortex, anterior, and subcallosal cingulate gyrus (Table 3 and Figure 5—blue peaks). The main effects analyses for IUP and WUP indicated that the hypothalamus (IUP = −12, −9, −3; z = 3.9; p = 0.001 SVC; WUP = 3, −15, −6; z = 3.5; p = 0.004 SVC), anterior insula/operculum (IUP = −39, 27, 3; z = 4.8; p = 0.0002; 36, 3, −3; z = 4.5; p = 0.0001 SVC; 39, 27,

Table 2. Results from Pleasant Analyses

Brain Region	x	y	z	z Statistic	p Value (after SVC)
IP + WP − tasteless					
Putamen	−27	12	−12	3.9	0.00001**
	27	9	−9	3.7	0.001
	27	*15*	*−15*	*3.4*	*0.002*
Claustrum	−30	12	−3	3.4	0.002
	−33	*3*	*−3*	*3.3*	*0.003*
Hypothalamus	0	−12	−12	4.3	0.0001
Thalamus (ventroposteromedial)	12	−27	6	4	0.0001
	9	*−24*	*9*	*3.9*	*0.0002*
Caudolateral orbitofrontal cortex/ anterior ventral insula	36	21	−21	4.6	0.00002**
Caudolateral orbitofrontal cortex	39	33	−18	4.0	0.04**
	−33	33	−21	3.4	0.002
Subcallosal cingulate cortex	−3	33	−6	3.6	0.001
Anterior cingulate cortex	0	39	6	4.7	0.0004**
	3	*42*	*−6*	*4.7*	*0.004*
IP – IUP					
Anterior cingulate cortex	−15	33	33	4.2	0.000008
Supplementary motor area	−12	36	38	4.0	0.03**
Caudolateral orbitofrontal cortex	39	33	−15	3.2	0.001
WP – WUP					
Ventral striatum	27	9	−12	4.4	0.00004
Caudolateral orbitofrontal cortex	39	31	−15	3.5	0.001

SVC, small volume correction; **cluster p value corrected for entire brain. Italics indicate that a peak falls under the same cluster as the preceding peak.

5; z = 4.3; p = 0.001 SVC; 27, 15, −15; z = 4.1; p = 0.001 SVC; WUP = 39, 33, −3; z = 3.9; p = 0.001 SVC; 42, 18, −15; z = 3.2; p = 0.002 SVC), orbitofrontal cortex (IUP = 42, 18, −12; z = 4.2; p = 0.0003 SVC; 9, 57, −21; z = 3.8; p = 0.001 SVC; WUP = −39, 15, −18; z = 4.4; p = 0.0002; 33, 27, −15; z = 3.8; 0.006), and anterior cingulate cortex (IUP = 9, 48, 30; z = 5.0; p = 0.0002; −3, 63, 18; z = 4.0; p = 0.0001; 9, 66, 6; z = 3.7; p = 0.002 SVC; WUP = 6, 42, 0; z = 4.3; p = 4×10^{-14}; 15, 9, 51; z = 3.8; p = 0.001 SVC; −12, 18, 45; z = 3.3; p = 0.001 SVC) were present in both conditions. Again in accordance with Anderson and colleagues (Anderson et al., 2003), the unpleasant taste activated the left orbitofrontal region, whereas the pleasant taste activated the right orbitofrontal region (Figures 5A–5C). However, while direct comparison of pleasant versus unpleasant (IP − IUP) and [(IP + WP) − (IUP + WUP)] isolated activation in the right caudolateral orbitofrontal region, the reverse contrasts did not isolate left orbitofrontal activity, nor was this region observed in IUP − IP or WUP − WP. Valence-specific effects were observed in the dorsal insula/opercular region with the intense unpleasant compared to the intense pleasant taste (IUP − IP) associated with greater activation in the left anterior dorsal insula/operculum (−39, 33, 0; z = 3.8; p = 0.0001 SVC) and the right mid dorsal insula/operculum (42, 0, 21; z = 4.2; p = 0.00008 SVC) showing greater activation in the weak unpleasant compared to weak pleasant taste (WUP − WP). These insular regions did not survive the direct comparison of both unpleasant solutions minus both pleasant solutions [(IUP + WP) – (IP + WP)], indicating a possible interaction with intensity rather than a response irrespective of intensity. A posterior region of anterior cingulate cortex was also activated more by WUP than WP.

Discussion

Sensory systems must code for a variety of interacting perceptual dimensions. By carefully equating pleasant and unpleasant gustatory stimuli for intensity, we were able to demonstrate functional segregation within the human gustatory system. We report that the cerebellum, pons, amygdala, and middle insula respond preferentially to taste intensity compared to affective valence (pleasant or unpleasant), whereas the anterior cingulate cortex, anterior ventral insula, and orbitofrontal cortex responded preferentially to both concentrations of a pleasant or unpleasant taste compared to a neutral tasteless solution (Figure 5). Valence-specific effects were found in the right caudolateral orbitofrontal cortex and anterior cingulate cortex, which responded preferentially to pleasant compared to unpleasant taste irrespective of intensity (Figure 5C). This result suggests that these regions may play a specific role in processing food-related chemosensory stimuli, since sweetness is commonly encountered in foods, whereas bitter perception tends to signify poison or spoilage. Although the left anterior orbitofrontal cortex, insula, and frontal operculum appeared in the comparison of both intensities of unpleasant taste to tasteless, only the anterior dorsal insula survived direct comparison of the intense unpleasant to intense pleasant taste, and no area survived the analysis probing regions responsive to unpleasant taste compared to pleasant taste irrespective of intensity. It is noteworthy that the left anterior dorsal insula/opercular region that responded best to intense unpleasant taste (Figure 5I) corresponds to the area identified by Phillips and colleagues as responding to facial expressions of disgust (Phillips et al., 1997). These parallel findings provide further support for Rozin's theory

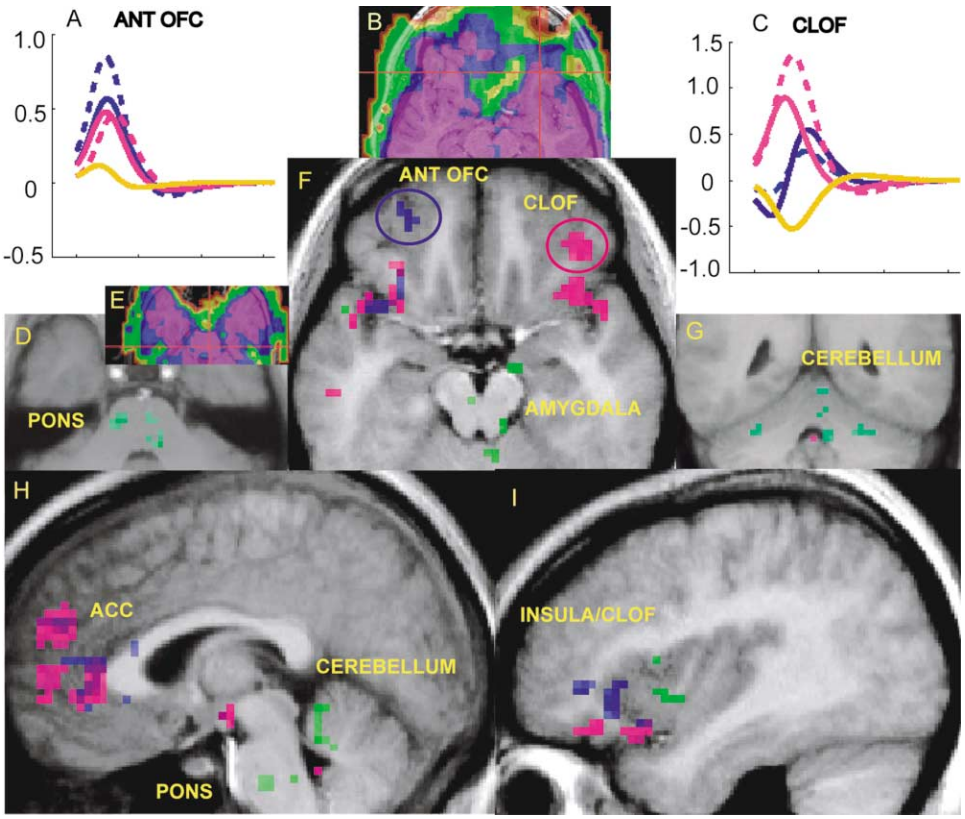

Figure 5. Dissociation of Taste Intensity and Affect

Results from the three main random effects analyses color coded and superimposed on the group mean image (D, F, G, H, and I) (green, intensity [(IP + IUP) − (WP + WUP)]; magenta, pleasant [(IP + WP) − tasteless]; blue, unpleasant [(IUP + WUP) − tasteless]). The activations highlight the dissociation between areas responsive to both concentrations of pleasant (magenta) or unpleasant (blue) taste versus those areas responsive to intensity irrespective of valence (green). Note the lack of intensity activation (green) throughout the orbitfrontal cortex (F) and anterior cingulate cortex (ACC) (H). Activation related to either pleasant (pink) or unpleasant (blue) taste is seen extending from the orbitofrontal cortex into the anterior ventral insula (I). In contrast, only activation related to intensity is observed in the middle insula (I), amygdala, pons (D), and cerebellum (G). The right graph (A) displays the fitted hrf extracted from the anterior orbitfrontal cortex region (ANT OFC) corresponding to the circled blue activation in the same representative subject (*y* axis, response; *x* axis, peristimulus time with each line indicating a 5 s interval). As per Figure 3, blue solid line, IUP; blue dotted line, WUP; magenta solid line, IP; magenta dotted line, WP; and yellow line, tasteless. Note that the response is greatest for WUP, illustrating that valence and not intensity drives the response in this region. The right graph (C) displays the fitted hemodynamic response function (hrf) extracted from the caudolateral orbitfrontal corresponding to the circled magenta activation in a representative subject (*y* axis, response; *x* axis, peristimulus time with each line indicating a 5 s interval). In (B), the BOLD detectability map for the orbitofrontal cortex is presented (Parrish et al., 2000), indicating that we are able to detect a 0.5%–1% signal change throughout a large portion of orbitofrontal cortex, although signal dropout is still evident within the caudomedial region. Purple indicates ability to detect a 0.5% signal change; blue, 1%; green, 2%; and yellow, 4%. The crosshatch is centered on the right caudolateral orbitfrontal cortex corresponding to the peak identified in [(IP + WP) − tasteless], which is activated to pleasant compared to unpleasant taste irrespective of valence. In (E), the BOLD detectability map is displayed for the brainstem, showing that we are able to detect greater than 0.5% signal change throughout this region.

that higher-order percepts of disgust evolved from the neural substrates for bad taste (Rozin and Fallon, 1987).

Dissociation of Response between the Amygdala and Orbitofrontal Cortex

Our results provide a striking replication of the recent findings of Anderson and colleagues, who used a similar paradigm to evaluate brain response to odor intensity and affect (Anderson et al., 2003). In both studies, response in the amygdala was associated with stimulus intensity irrespective of affective valence, whereas a valence-specific response for pleasant taste irrespective of intensity was identified in the right orbitofrontal cortex. Anderson and colleagues also noted activation in the left anterior orbitofrontal cortex to an unpleasant odor (Figures 5A, 5C, and 5F). We observed activation in this same area to the unpleasant tastes compared to the tasteless condition, but it did not survive a direct comparison to the pleasant tastes. Interestingly, Zald and colleagues recently reported a reanalysis of their amygdala activation to unpleasant odors, noting a positive relationship with perceived odor intensity in the amygdala but not the orbitofrontal cortex (Zald, 2003b).

Clearly, in both studies, amygdalar response was driven primarily by intensity. This calls into question the notion that the amygdala "tags" sensory stimuli with an affective label. However, we also note that deactivations were observed in the amygdala to the weak unpleasant

Table 3. Results from Unpleasant Analyses

Brain Region	x	y	z	z Statistic	p Value (after SVC)
IUP + WUP − tasteless					
Midbrain	−3	−27	−12	3.5	0.002
Hypothalamus	−9	−9	−6	3.7	0.001
	0	*−9*	*−12*	*3.5*	*0.002*
Claustrum	−30	3	9	5.0	0.00002
	33	6	9	4.5	0.00002
Insula/operculum	−39	6	−6	4.5	3×10^{-13}**
	−54	*9*	*9*	*4.2*	*0.004*
	−48	*12*	*0*	*4.2*	*0.004*
	−45	*18*	*−9*	*4.1*	*0.005*
	45	−3	−12	4.4	0.00005
	−39	27	−3	3.5	0.001
	39	15	−15	3.4	0.002
	−27	48	−18	3.9	0.001
Anterior orbitofrontal cortex	*−30*	*42*	*−15*	*3.4*	*0.004*
	6	54	21	4.4	0.001
Anterior cingulate cortex/ medial prefrontal cortex	*3*	*45*	*−3*	*4.3*	*0.002*
	6	24	15	4.0	0.0002
	−6	21	30	3.9	0.001
	−12	*18*	*45*	*3.5*	*0.002*
	−15	48	24	3.9	0.001
	9	39	36	3.8	0.003
	6	30	−9	3.4	0.002
Subcallosal cingulate	45	42	−6	4.6	2×10^{-8}**
	39	*27*	*−9*	*4.2*	*0.002*
Ventral lateral prefrontal cortex	−48	36	−9	3.7	0.001**
	−24	51	0	3.7	0.00002**
IUP − IP					
Cerebellum	−30	−51	−27	3.3	0.002
Posterior insula	36	−9	15	3.8	0.001
Dorsal insula/operculum	−39	33	0	3.8	0.001
Ventral lateral prefrontal cortex/ frontal operculum	54	21	−9	3.8	0.001
WUP − WP					
Frontal operculum	42	0	21	4.2	0.00008
Posterior anterior cingulate cortex	−18	−6	39	3.9	0.0002
	15	6	38	3.7	0.001

SVC, small volume correction; **cluster p value corrected for entire brain. Italics indicate that a peak falls under the same cluster as the preceding peak.

taste but not to the weak pleasant taste. This suggests that amygdaloid activity is best characterized by a complex interaction between valence and intensity, which is consistent with its previously described heterogeneity in structure and function (Aggleton et al., 1980; Amaral et al., 1992; Baxter and Murray, 2002; Zald, 2003a).

Studies that show amygdala activation without perceptual awareness (and thus possessing zero perceptual intensity) also argue against a straightforward role for the amygdala in stimulus intensity coding (Morris et al., 1999). Other evidence for a complex interaction of intensity and valence within the gustatory modality comes from two studies of patients with excision from the anterior temporal lobe for the treatment of intractable epilepsy (Small et al., 2001b, 2001c). In both studies, the patients displayed increased intensity perception for aversive but not for pleasant taste. In these studies, the surgeries always included radical resection of the amygdala, and deficits were attributed to the amygdala lesions, since taste-responsive cells that are sensitive to intensity have been recorded from the primate amygdala (Scott et al., 1993).

Flavor novelty may also be dependent upon processing within the amygdala. In an earlier study, we used positron emission tomography to measure brain response to presentation of a series of tastes/odor pairs (Small et al., 1997). In one 60 s scan, subjects were presented sequentially with tastes and smells that "matched" (a sweet taste with a strawberry odor followed by a salty taste with a soy sauce odor, etc.). In a separate scan, subjects were presented with the same tastes and smells in mismatched pairings (a sweet taste with a soy sauce smell followed by a salty taste with a strawberry odor). In both scans, identical stimuli were presented and thus concentration was perfectly controlled. Nevertheless, amygdala activation was observed in the mismatched condition, which was described as unpleasant and unfamiliar, compared to the matched condition, described as pleasant and familiar. Although we did not ask our subjects to judge intensity, based upon the fact that unpleasant tastes are generally judged as more intense than pleasant tastes, irrespective of concentration (Pfaffmann, 1980; Pfaffmann et al., 1977), we predict that the increase in novelty and unpleasantness was also accompanied by the experience of greater intensity. Future studies will be important in dissecting

the brain substrates differentiating subjective intensity perception from physical differences in stimulus concentration, but we suspect that the integrated coding in the amygdala for intensity, novelty, and affective tone may play a key role in this dissociation.

Given the aforementioned findings, we favor the interpretation that the amygdala is important in establishing the saliency of sensory stimuli, which is determined by the interacting dimensions of intensity, valence, and perhaps novelty/familiarity. One important function of this integrated coding may be in biasing processing in favor of adaptive needs so that subjective experience can be released from dependence upon physical attributes of the stimulus.

The finding of valence-specific responses in the orbitofrontal cortex is in accordance with a whole literature on reward processing in this region (Montague and Berns, 2002; Rolls, 2000; Schultz et al., 2000; Tremblay and Schultz, 2000). The finding is also consistent with previous chemosensory studies showing that the orbitofrontal cortex and not the amygdala responds to changes in pleasantness associated with eating (O'Doherty et al., 2000; Rolls et al., 1989; Small et al., 2001a). The orbitofrontal cortex is also the only region of the brain to respond to the receipt and anticipation of both pleasant and unpleasant taste (O'Doherty et al., 2002).

Although several studies have investigated brain response to pleasant and unpleasant tastes (O'Doherty et al., 2001b; Zald et al., 1998, 2002), none have equated stimuli for intensity, and no study has yet examined brain response to taste intensity. Zald has noted that the left orbitofrontal cortex is more frequently activated by unpleasant chemosensation, whereas the right orbitofrontal cortex is more frequently activated by pleasant chemosensation (Zald and Pardo, 2000). Our results are consistent with this observation, since we observed activations occurring predominantly on the right in the pleasantness analyses and predominantly on the left in the unpleasantness analyses. These results are unlikely due to differences in intensity since the stimuli were matched for intensity, and no intensity-related activation was observed in the orbitofrontal region in the intensity analyses (Figure 4).

It is also noteworthy that the right hemisphere activation corresponded well to the human anatomical homolog of the secondary gustatory area (Small et al., 1999), whereas the left hemisphere activations tended to be more anterior. This suggests that the asymmetry may not be a function of valence per se (pleasantness versus unpleasantness) but rather related to subfunctions of the orbitofrontal cortex, such as flavor processing (most pleasant tastes and smells are edible whereas unpleasant stimuli are not) versus processing of danger or avoidance (most poisonous substances are bitter).

Dissociation in the Gustatory System

As noted above, the orbitofrontal cortex, which represents the secondary gustatory region, responds to the affective qualities and not the intensity of the taste stimuli. Single-cell recording studies show that taste-responsive cells in the amygdala (Scott et al., 1993) and primary gustatory area are responsive to the concentration of a taste solution (Scott and Plata-Salaman, 1999; Scott et al., 1986a, 1986b). Our results indicate that these same regions are associated with taste intensity perception in humans. However, the amygdala activation observed here was further posterior to the region where Scott and colleagues were recording (Figure 3A). The analysis of BOLD detectability within the amygdala indicates that this discrepancy is unlikely related to a reduced ability to measure signal from more anterior portions of the amygdala (Figure 3D). While the exact location of amygdala activity varied quite a bit between subjects, the region isolated in the group analysis is almost identical to the region Anderson and colleagues reported as sensitive to odor intensity (Anderson et al., 2003). It is therefore possible that the region of the amygdala coding for chemosensory intensity differs in humans and primates. In contrast, the region of insula/operculum that responded to intensity is roughly homologous to the insula/opercular region from which Scott and colleagues record in primates (Figure 4). However, since the posterior insula and overlying operculum has also been proposed as a candidate for the primary gustatory area (Kobayakawa et al., 1999), we lowered the threshold of our activation map to 0.005. This enabled us to see a small activation within this region that was not visible at 0.001. Nevertheless, our data clearly show that the middle insula and overlying frontal operculum are more sensitive to stimulus intensity. This same area has also been shown to respond to electrically induced taste perception (Barry et al., 2001).

We were also able to identify an insular region that appeared most sensitive to the affective quality of taste. This region extended from the middle insula ventrally toward the caudal orbitofrontal cortex (Figures 5F and 5I) and was relatively insensitive to taste intensity perception. The possibility of multiple gustatory representations within the insula/operculum has been previously proposed in rats (Scott and Plata-Salaman, 1999; Small et al., 1999; Yamamoto et al., 1980, 1984) and primates (Pritchard et al., 1986). The current results suggest a division of function within these regions.

Finally, the parabrachial region of the pons was the most sensitive region in the brain to taste intensity (Figures 5D and 5H). In rats, the pontine parabrachial nucleus represents a second-order taste relay, and the gustatory responses have been well characterized (Di Lorenzo, 1988, 1989, 1990; Di Lorenzo and Monroe, 1989; Di Lorenzo and Schwartzbaum, 1982; Norgren and Pfaffmann, 1975; Sclafani et al., 2001; Spector, 1995). Despite several attempts, a pontine taste relay has not been identified in nonhuman primates (Norgren, 1990), and although its existence has been postulated, its role in gustatory processing is suggested to be minimal (Norgren, 1990). In humans, there are a handful of reports of taste disturbances following pontine lesions (Fujikane et al., 1998; Kojima and Hirano, 1999; Sato and Nitta, 2000). Although further studies are needed, our finding is highly suggestive of a role for the pons in taste intensity coding in humans.

Beyond the Gustatory System

The cerebellum and anterior cingulate cortex are not considered part of the gustatory system, yet responses within these regions are observed in most neuroimaging

studies of taste and smell (Barry et al., 2001; Kinomura et al., 1994; O'Doherty et al., 2001b; Poellinger et al., 2001; Small et al., 1997, 2001a; Sobel et al., 1998, 2000; Yousem et al., 2001; Zald et al., 1998, 2002; Zald and Pardo, 1997). The anterior cingulate cortex was activated by all tastes (Figure 5H) but responded preferentially to the pleasant taste. A similar region was also shown to be be activated by pleasurable touch (Francis et al., 1999) and pain (Hofbauer et al., 2001) irrespective of intensity, suggesting a role for this region in affective processing of many sensory stimuli. It is not immediately clear what the cerebellar response is contributing to taste intensity coding (Figures 5G and 5H). However, our finding is consistent with a previous report of a positive relationship between odor concentration and cerebellar activation (Sobel et al., 1998). Sobel and colleagues also found activation related to sniff volume and suggested that the cerebellum is important in coordinating sniff volume with respect to stimulus intensity. It is therefore possible that the cerebellum uses information about taste intensity to guide oral movements during eating.

In summary, our results support a functional segregation within the human gustatory system, with the pons and middle insula coding for stimulus intensity and the anteroventral insula, dorsal insula/operculum, caudolateral orbitofrontal, and anterior cingulate cortex coding for affective valuation. Our results also cast further doubt upon the notion that the amygdala is specialized for processing unpleasant sensory stimuli or determining affective valence. Instead, we found that amygdala activation was driven by stimulus intensity, whereas valence-specific responses were found in the anterior cingulate cortex and caudolateral orbitfrontal cortex. These results suggest that hedonic stimuli will produce markedly different responses depending upon perceived intensity and underline the importance of considering the interacting nature of valence and intensity in trying to understand affective coding of sensory stimuli.

Experimental Procedures

Subjects

The Institutional Review Board at Northwestern University approved the study protocol. Nineteen healthy volunteers gave written informed consent and participated in a screening and training session in which they rated the intensity and pleasantness of several concentrations of sweet and bitter solutions. Ratings within the target range were obtained for all but four subjects, who were subsequently excluded. Of the remaining 15 subjects, six were excluded either because movements made during scanning surpassed a predetermined acceptable limit (>1 cm movement in any direction in more than one scan) or due to technical difficulties with either the scanner or gustometer. Of the remaining nine, six were women, and the mean age was 24 years. All subjects reported being right handed, and all were classified as being right handed by the modified Edinburgh inventory (Oldfield, 1971). The average handedness score was 87 out of a possible 100. All subjects were of average weight and screened for obesity and malnutrition on the basis of their body mass index. All subjects also reported no known taste, smell, neurological, or psychiatric disorder. Finally, subjects were also asked to rate the intensity of papers soaked in 6-n-Propylthiouracil (PROP) using the general labeled magnitude scale (Green et al., 1996) to determine taster status (Prutkin et al., 2000). The mean PROP was 45 with a standard deviation of 21. All subjects were classified as "tasters," except one whose score fell in the nontaster range. There were no supertasters in the group.

Procedures

Chemosensory Laboratory

Subjects sampled and rated the intensity and pleasantness/unpleasantness of five concentrations of sucrose (ranging from 1.8 to 5.6×10^{-2} M) and quinine sulfate (ranging from 1.0×10^{-3} to 1.0×10^{-5}) using an 11 point scale (Figure 1). Solutions were delivered as a 0.5 cc bolus from a calibrated dropping pipette. Concentrations with ratings falling in the targeted range (Figure 1) were selected as stimuli for use in the fMRI experiment.

fMRI Scanner

A slow event-related paradigm was used to image brain responses to each of the five events (IP, IUP, WP, WUP, and tasteless) (Figure 2). The images were acquired on a Siemen's 1.5 Tesla Sonata scanner. Echoplanar imaging was used to measure the blood oxygenation-level dependent (BOLD) signal as an indication of cerebral brain activation. A susceptibility-weighted single-shot echoplanar method was used to image the regional distribution of the BOLD signal with TR, 2100 ms; TE, 40 ms; flip angle, 90°; FOV, 240 mm; matrix, 64×64; slice thickness, 4 mm; and acquisition of 28 contiguous slices. Slices were acquired in an interleaved mode to reduce the crosstalk of the slice selection pulse. At the beginning of each functional run, the MR signal was allowed to equilibrate over six scans for a total of 12.6 s, which was then excluded from analysis. The anatomical scan used a T1-weighted 3D FLASH sequence (TR/TE, 20/6 ms; flip angle, 20°; matrix, 256×256; 1 mm thick slices; fov, 240; 160 slices) and a saturation slab was placed inferior to the imaging slab to reduce the blood flow artifact in the temporal lobes. A signal to noise map in the amygdala, orbitofrontal cortex, and pons was generated (amygdala displayed in Figure 3, and OFC displayed in Figure 4). The images indicated that we were able to detect 0.5%–1% signal changes in all three regions, except the caudomedial portion of the orbitofrontal cortex.

fMRI Data Analysis

Data were analyzed on UNIX/LINUX workstations under the Matlab Software (MathWorks, Inc., Sherborn, MA) using SPM99 (Wellcome Department of Cognitive Neurology, London, UK). Functional images were time acquisition corrected to the slice obtained at 50% of the TR. All functional images were then realigned to the scan immediately preceding the anatomical T1 image. The images (anatomical and functional) were then normalized to the Montreal Neurological Institute template (MNI-305), which approximates the anatomical space delineated by Talairach and Tournoux (Talairach and Tournoux, 1988). Functional images were smoothed with a 7 mm FWHM isotropic Gaussian kernel. For time-series analysis on all subjects, a high-pass filter was included in the filtering matrix (according to convention in SPM99) in order to remove low-frequency noise and slow drifts in the signal, which could bias the estimates of the error. Condition-specific effects at each voxel were estimated using the general linear model. The response to events was modeled by a canonical hemodynamic response function (HRF), consisting of a mixture of 2 γ functions that emulate the early peak at 5 s and the subsequent undershoot. The temporal derivative of the hemodynamic function was also included as part of the basis set to enable examination of differences in timing between various events (Henson et al., 2002).

Within-group comparisons were performed using a conjunction analysis within a fixed-effects model for one comparison [(IP + WP) and (IUP + WUP)] and random-effects models for all other comparisons in order to account for intersubject variability. Parameter estimate images from designated contrasts (e.g., strong sucrose versus weak sucrose) were entered into second-level analyses using one-sample Student's t tests. SPM assigns significance t fields from all analyses using the theory of Gaussian random fields (Friston et al., 1995; Worsley and Friston, 1995). Activations that were not predicted were considered significant at $p \leq 0.05$ at the cluster level after correction for multiple comparisons across all voxels. Predicted peaks were considered significant at $p \leq 0.005$ within regions of interest, specified a priori, and probed for significance by small volume corrections to the nearest cluster. Finally, region of interest analyses were carried out for the right caudolateral orbitofrontal cortex, anterior cingulate, left anterior orbitofrontal cortex, and insula in the comparison of (IP + WP) − (IUP + WUP) or its inverse, using a 5 mm sphere around peaks identified in the primary random effects analyses (IP + WP − tasteless) and (IUP + WUP − tasteless) and the MARSBAR tool available for use within SPM99.

Acknowledgments

This work was supported by funds awarded to D.M.S. from the Cognitive Neurology and Alzheimer's Disease Center and grant AG0094 awarded to D.G. by the National Institute of Aging. We would like to thank Brittany Lapin and Katherine Simmons for their help on this project; and three anonymous reviewers for their constructive comments, which we feel strengthened the manuscript considerably.

Received: March 27, 2003
Revised: May 6, 2003
Accepted: July 3, 2003
Published: August 13, 2003

References

Aggleton, J.P., Burton, M.J., and Passingham, R.E. (1980). Cortical and subcortical afferents to the amygdala of the rhesus monkey (*Macaca mulatta*). Brain Res. *190*, 347–368.

Amaral, D.G., Price, J.L., Pitkanen, A., and Carmichael, S.T. (1992). Anatomical organization of the primate amygdaloid complex. In The Amygdala: Neurobiological Aspects of Emotion, Memory, and Mental Dysfunction, J.P. Aggleton, ed. (New York: Wile-Liss), pp. 1–66.

Anderson, A.K., Christoff, K., Stappen, I., Panitz, D., Ghahremani, D.G., Glover, G., Gabrieli, J.D.E., and Sobel, N. (2003). Dissociated neural representations of intensity and valence in human olfaction. Nat. Neurosci. *6*, 196–202.

Apkarian, A.V., Darbar, A., Krauss, B.R., Gelnar, P.A., and Szeverenyi, N.M. (1999). Differentiating cortical areas related to pain perception from stimulus identification: temporal analysis of fMRI activity. J. Neurophysiol. *81*, 2956–2963.

Apkarian, A.V., Gelnar, P.A., Krauss, B.R., and Szeverenyi, N.M. (2000). Cortical responses to thermal pain depend on stimulus size: a functional MRI study. J. Neurophysiol. *83*, 3113–3122.

Apkarian, A.V., Krauss, B.R., Fredrickson, B.E., and Szeverenyi, N.M. (2001). Imaging the pain of low back pain: functional magnetic resonance imaging in combination with monitoring subjective pain perception allows the study of clinical pain states. Neurosci. Lett. *299*, 57–60.

Barry, M.A., Gatenby, J.C., Zeiger, J.D., and Gore, J.C. (2001). Hemispheric dominance of cortical activity evoked by focal electrogustatory stimuli. Chem. Senses *26*, 471–482.

Baxter, M.G., and Murray, E.A. (2002). The amygdala and reward. Nat. Rev. Neurosci. *3*, 563–573.

Berns, G.S., McClure, S.M., Pagnoni, G., and Montague, P.R. (2001). Predictability modulates human brain response to reward. J. Neurosci. *21*, 2793–2798.

Blood, A.J., and Zatorre, R.J. (2001). Intensely pleasurable responses to music correlate with activity in brain regions implicated in reward and emotion. Proc. Natl. Acad. Sci. USA *98*, 11818–11823.

Blood, A.J., Zatorre, R.J., Bermudez, P., and Evans, A.C. (1999). Emotional responses to pleasant and unpleasant music correlate with activity in paralimbic brain regions. Nat. Neurosci. *2*, 382–387.

Carretie, L., Mercado, F., Tapia, M., and Hinojosa, J.A. (2001). Emotion, attention, and the 'negativity bias', studied through event-related potentials. Int. J. Psychophysiol. *41*, 75–85.

Di Lorenzo, P.M. (1988). Taste responses in the parabrachial pons of decerebrate rats. J. Neurophysiol. *59*, 1871–1887.

Di Lorenzo, P.M. (1989). Across unit patterns in the neural response to taste: vector space analysis. J. Neurophysiol. *62*, 823–833.

Di Lorenzo, P.M. (1990). Corticofugal influence on taste responses in the parabrachial pons of the rat. Brain Res. *530*, 73–84.

Di Lorenzo, P.M., and Schwartzbaum, J.S. (1982). Coding of gustatory information in the pontine parabrachial nuclei of the rabbit: magnitude of neural response. Brain Res. *251*, 229–244.

Di Lorenzo, P.M., and Monroe, S. (1989). Taste responses in the parabrachial pons of male, female and pregnant rats. Brain Res. Bull. *23*, 219–227.

Francis, S., Rolls, E.T., Bowtell, R., McGlone, F., O'Doherty, J., Browning, A., Clare, S., and Smith, E. (1999). The representation of pleasant touch in the brain and its relationship with taste and olfactory areas. Neuroreport *10*, 435–459.

Friston, K.J., Jezzard, P., and Turner, R. (1994). Analysis of functional MRI time-series. Hum. Brain Mapp. *1*, 153–171.

Friston, K.J., Holmes, A.P., Worsley, K.J., Poline, J.B., Frith, C.D., and Frackowiak, R.S.J. (1995). Statistical parametric maps in functional imaging. Hum. Brain Mapp. *2*, 189–210.

Fujikane, M., Nakazawa, M., Ogasawara, M., Hirata, K., and Tsudo, N. (1998). Unilateral gustatory disturbance by pontine infarction. Rinsho Shinkeigaku *38*, 342–343.

Green, B.G., Dalton, P., Cowart, B., Shaffer, G., Rankin, K., and Higgins, J. (1996). Evaluating the 'Labeled Magnitude Scale' for measuring sensations of taste and smell. Chem. Senses *21*, 323–334.

Henson, R.N., Price, C.J., Rugg, M.D., Turner, R., and Friston, K.J. (2002). Detecting latency differences in event-related BOLD responses: application to words versus nonwords and initial versus repeated face presentations. Neuroimage *15*, 83–97.

Hofbauer, R.K., Rainville, P., Duncan, G.H., and Bushnell, M.C. (2001). Cortical representation of the sensory dimension of pain. J. Neurophysiol. *86*, 402–411.

Kinomura, S., Kawashima, R., Yamada, K., Ono, S., Itoh, M., Yoshioka, S., Yamaguchi, T., Matsui, H., Miyazawa, H., and Itoh, H. (1994). Functional anatomy of taste perception in the human brain studied with positron emission tomography. Brain Res. *659*, 263–266.

Kobayakawa, T., Ogawa, H., Kaneda, H., Ayabe-Kanamura, S., Endo, H., and Saito, S. (1999). Spatio-temporal analysis of cortical activity evoked by gustatory stimulation in humans. Chem. Senses *24*, 201–209.

Kojima, Y., and Hirano, T. (1999). A case of gustatory disturbance caused by ipsilateral pontine hemorrhage. Rinsho Shinkeigaku *39*, 979–981.

LaBar, K.S., Gitelman, D.R., Parrish, T.B., Kim, Y.H., Nobre, A.C., and Mesulam, M.M. (2001). Hunger selectively modulates corticolimbic activation to food stimuli in humans. Behav. Neurosci. *115*, 493–500.

Lane, R.D., Reiman, E.M., Bradley, M.M., Lang, P.J., Ahern, G.L., Davidson, R.J., and Schwartz, G.E. (1997). Neuroanatomical correlates of pleasant and unpleasant emotion. Neuropsychologia *35*, 1437–1444.

Montague, P.R., and Berns, G.S. (2002). Neural economics and the biological substrates of valuation. Neuron *36*, 265–284.

Morris, J.S., Friston, K.J., and Dolan, R.J. (1997). Neural responses to salient visual stimuli. Proc. R. Soc. Lond. B Biol. Sci. *264*, 769–775.

Morris, J.S., Ohman, A., and Dolan, R.J. (1999). A subcortical pathway to the right amygdala mediating "unseen" fear. Proc. Natl. Acad. Sci. USA *96*, 1680–1685.

Norgren, R. (1990). Gustatory system. In The Human Nervous System, G. Paxinos, ed. (San Diego: Academic Press), pp. 845–861.

Norgren, R., and Pfaffmann, C. (1975). The pontine taste area in the rat. Brain Res. *91*, 99–117.

O'Doherty, J., Rolls, E.T., Francis, S., Bowtell, R., McGlone, F., Kobal, G., Renner, B., and Ahne, G. (2000). Sensory-specific satiety-related olfactory activation of the human orbitofrontal cortex. Neuroreport *11*, 893–897.

O'Doherty, J., Kringelbach, M.L., Rolls, E.T., Hornak, J., and Andrews, C. (2001a). Abstract reward and punishment representations in the human orbitofrontal cortex. Nat. Neurosci. *4*, 95–102.

O'Doherty, J., Rolls, E.T., Francis, S., Bowtell, R., and McGlone, F. (2001b). Representation of pleasant and aversive taste in the human brain. J. Neurophysiol. *85*, 1315–1321.

O'Doherty, J.P., Deichmann, R., Critchley, H.D., and Dolan, R.J. (2002). Neural responses during anticipation of a primary taste reward. Neuron *33*, 815–826.

Oldfield, R.C. (1971). The assessment and analysis of handedness: the Edinburgh inventory. Neuropsychologia *9*, 97–113.

Parrish, T.B., Gitelman, D.R., LaBar, K.S., and Mesulam, M.M. (2000).

Impact of signal-to-noise on functional MRI. Magn. Reson. Med. *44*, 925–932.

Petrides, M., and Pandya, D. (1994). Comparitive architectonic analysis of the human and macaque frontal cortex. In Handbook of Neuropsychology, F. Boller and J. Grafman, eds. (Amsterdam: Elsevier), pp. 17–58.

Pfaffmann, C. (1980). Wundt's schema of sensory affect in the light of research on gustatory preferences. Psychol. Res. *42*, 165–174.

Pfaffmann, C., Norgren, R., and Grill, H.J. (1977). Sensory affect and motivation. Ann. N Y Acad. Sci. *290*, 18–34.

Phillips, M.L., Young, A.W., Senior, C., Brammer, M., Andrew, C., Calder, A.J., Bullmore, E.T., Perrett, D.I., Rowland, D., Williams, S.C., et al. (1997). A specific neural substrate for perceiving facial expressions of disgust. Nature *389*, 495–498.

Poellinger, A., Thomas, R., Lio, P., Lee, A., Makris, N., Rosen, B.R., and Kwong, K.K. (2001). Activation and habituation in olfaction–an fMRI study. Neuroimage *13*, 547–560.

Pritchard, T.C., Hamilton, R.B., Morse, J.R., and Norgren, R. (1986). Projections of thalamic gustatory and lingual areas in the monkey, *Macaca fascicularis*. J. Comp. Neurol. *244*, 213–228.

Prutkin, J., Fisher, E.M., Etter, L., Fast, K., Gardner, E., Lucchina, L.A., Snyder, D.J., Tie, K., Weiffenbach, J., and Bartoshuk, L.M. (2000). Genetic variation and inferences about perceived taste intensity in mice and men. Physiol. Behav. *69*, 161–173.

Rolls, E.T. (2000). The orbitofrontal cortex and reward. Cereb. Cortex *10*, 284–294.

Rolls, E.T., Sienkiewicz, Z.J., and Yaxley, S. (1989). Hunger modulates the responses to gustatory stimuli of single neurons in the caudolateral orbitofrontal cortex of the macaque monkey. Eur. J. Neurosci. *1*, 53–70.

Royet, J.P., Zald, D., Versace, R., Costes, N., Lavenne, F., Koenig, O., and Gervais, R. (2000). Emotional responses to pleasant and unpleasant olfactory, visual, and auditory stimuli: a positron emission tomography study. J. Neurosci. *20*, 7752–7759.

Rozin, P., and Fallon, A.E. (1987). A persepective on disgust. Psychol. Rev. *94*, 23–41.

Sato, K., and Nitta, E. (2000). A case of ipsilateral ageusia, sensorineural hearing loss and facial sensorimotor disturbance due to pontine lesion. Rinsho Shinkeigaku *40*, 487–489.

Schultz, W., Tremblay, L., and Hollerman, J.R. (2000). Reward processing in primate orbitofrontal cortex and basal ganglia. Cereb. Cortex *10*, 272–284.

Sclafani, A., Azzara, A.V., Touzani, K., Grigson, P.S., and Norgren, R. (2001). Parabrachial nucleus lesions block taste and attenuate flavor preference and aversion conditioning in rats. Behav. Neurosci. *115*, 920–933.

Scott, T.R., and Plata-Salaman, C.R. (1999). Taste in the monkey cortex. Physiol. Behav. *67*, 489–511.

Scott, T.R., Yaxley, S., Sienkiewicz, Z.J., and Rolls, E.T. (1986a). Gustatory responses in the frontal opercular cortex of the alert cynomolgus monkey. J. Neurophysiol. *56*, 876–890.

Scott, T.R., Yaxley, S., Sienkiewicz, Z.J., and Rolls, E.T. (1986b). Gustatory responses in the nucleus tractus solitarius of the alert cynomolgus monkey. J. Neurophysiol. *55*, 182–200.

Scott, T.R., Karadi, Z., Oomura, Y., Nishino, H., Plata-Salaman, C.R., Lenard, L., Giza, B.K., and Aou, S. (1993). Gustatory neural coding in the amygdala of the alert macaque monkey. J. Neurophysiol. *69*, 1810–1820.

Small, D.M., Jones-Gotman, M., Zatorre, R.J., Petrides, M., and Evans, A.C. (1997). Flavor processing: more than the sum of its parts. Neuroreport *8*, 3913–3917.

Small, D.M., Zald, D.H., Jones-Gotman, M., Zatorre, R.J., Pardo, J.V., Frey, S., and Petrides, M. (1999). Human cortical gustatory areas: a review of functional neuroimaging data. Neuroreport *10*, 7–14.

Small, D.M., Zatorre, R.J., Dagher, A., Evans, A.C., and Jones-Gotman, M. (2001a). Changes in brain activity related to eating chocolate: from pleasure to aversion. Brain *124*, 1720–1733.

Small, D.M., Zatorre, R.J., and Jones-Gotman, M. (2001b). Changes in taste intensity perception following anterior temporal lobe removal in humans. Chem. Senses *26*, 425–432.

Small, D.M., Zatorre, R.J., and Jones-Gotman, M. (2001c). Increased intensity perception of aversive taste following right anteromedial temporal lobe removal in humans. Brain *124*, 1566–1575.

Sobel, N., Prabhakaran, V., Hartley, C.A., Desmond, J.E., Zhao, Z., Glover, G.H., Gabrieli, J.D., and Sullivan, E.V. (1998). Odorant-induced and sniff-induced activation in the cerebellum of the human. J. Neurosci. *18*, 8990–9001.

Sobel, N., Prabhakaran, V., Zhao, Z., Desmond, J.E., Glover, G.H., Sullivan, E.V., and Gabrieli, J.D. (2000). Time course of odorant-induced activation in the human primary olfactory cortex. J. Neurophysiol. *83*, 537–551.

Spector, A.C. (1995). Gustatory function in the parabrachial nuclei: implications from lesion studies in rats. Rev. Neurosci. *6*, 143–175.

Stoleru, S., Gregoire, M.C., Gerard, D., Decety, J., Lafarge, E., Cinotti, L., Lavenne, F., LeBars, D., Vernet-Maury, E., Rada, H., et al. (1999). Neuroanatomical correlates of visually evoked sexual arousal in human males. Arch. Sex. Behav. *28*, 1–21.

Talairach, J., and Tournoux, P. (1988). Co-Planar Stereotaxic Atlas of the Human Brain (New York: Thieme).

Thut, G., Schultz, W., Roelcke, U., Nienhusmeier, M., Missimer, J., Maguire, R.P., and Leenders, K.L. (1997). Activation of the human brain by monetary reward. Neuroreport *8*, 1225–1228.

Tremblay, L., and Schultz, W. (2000). Modifications of reward expectation-related neuronal activity during learning in primate orbitofrontal cortex. J. Neurophysiol. *83*, 1877–1885.

Worsley, K.J., and Friston, K.J. (1995). Analysis of fMRI time-series revisited–again. Neuroimage *2*, 173–181.

Worsley, K.J., Marrett, S., Neelin, P., Vandal, A.C., Friston, K.J., and Evans, A.C. (1996). A unified statistical approach for determining significant signals in images of cerebral activation. Hum. Brain Mapp. *4*, 58–73.

Yamamoto, T., Matsuo, R., and Kawamura, Y. (1980). Localization of cortical gustatory area in rats and its role in taste discrimination. J. Neurophysiol. *44*, 440–455.

Yamamoto, T., Yuyama, N., Kato, T., and Kawamura, Y. (1984). Gustatory responses of cortical neurons in rats. I. Response characteristics. J. Neurophysiol. *51*, 616–635.

Yousem, D.M., Oguz, K.K., and Li, C. (2001). Imaging of the olfactory system. Semin. Ultrasound CT MR *22*, 456–472.

Zald, D. (2003a). The human amgydala and the emotional evalutation of sensory stimuli. Brain Res. Rev. *41*, 88–123.

Zald, D. (2003b). Neuroimaging the dynamic interplay of emotion and olfaction. Paper presented at: Association for chemoreception sciences XXV (Sarasotta, Florida: Chemical Senses).

Zald, D.H., and Pardo, J.V. (1997). Emotion, olfaction, and the human amygdala: amygdala activation during aversive olfactory stimulation. Proc. Natl. Acad. Sci. USA *94*, 4119–4124.

Zald, D.H., and Pardo, J.V. (2000). Functional neuroimaging of the olfactory system in humans. Int. J. Psychophysiol. *36*, 165–181.

Zald, D.H., Lee, J.T., Fluegel, K.W., and Pardo, J.V. (1998). Aversive gustatory stimulation activates limbic circuits in humans. Brain *121*, 1143–1154.

Zald, D.H., Hagen, M.C., and Pardo, J.V. (2002). Neural correlates of tasting concentrated quinine and sugar solutions. J. Neurophysiol. *87*, 1068–1075.